

12-3-93  
P.36

NASA Technical Memorandum 105993  
ICOMP-92-27; CMOTT-92-14

# A Realizable Reynolds Stress Algebraic Equation Model

Tsan-Hsing Shih and Jiang Zhu  
*Institute for Computational Mechanics in Propulsion  
and Center for Modeling of Turbulence and Transition  
NASA Lewis Research Center  
Cleveland, Ohio*

and

John L. Lumley  
*Cornell University  
Ithaca, New York*

(NASA-TM-105993) A REALIZABLE  
REYNOLDS STRESS ALGEBRAIC EQUATION  
MODEL (NASA) 36 p

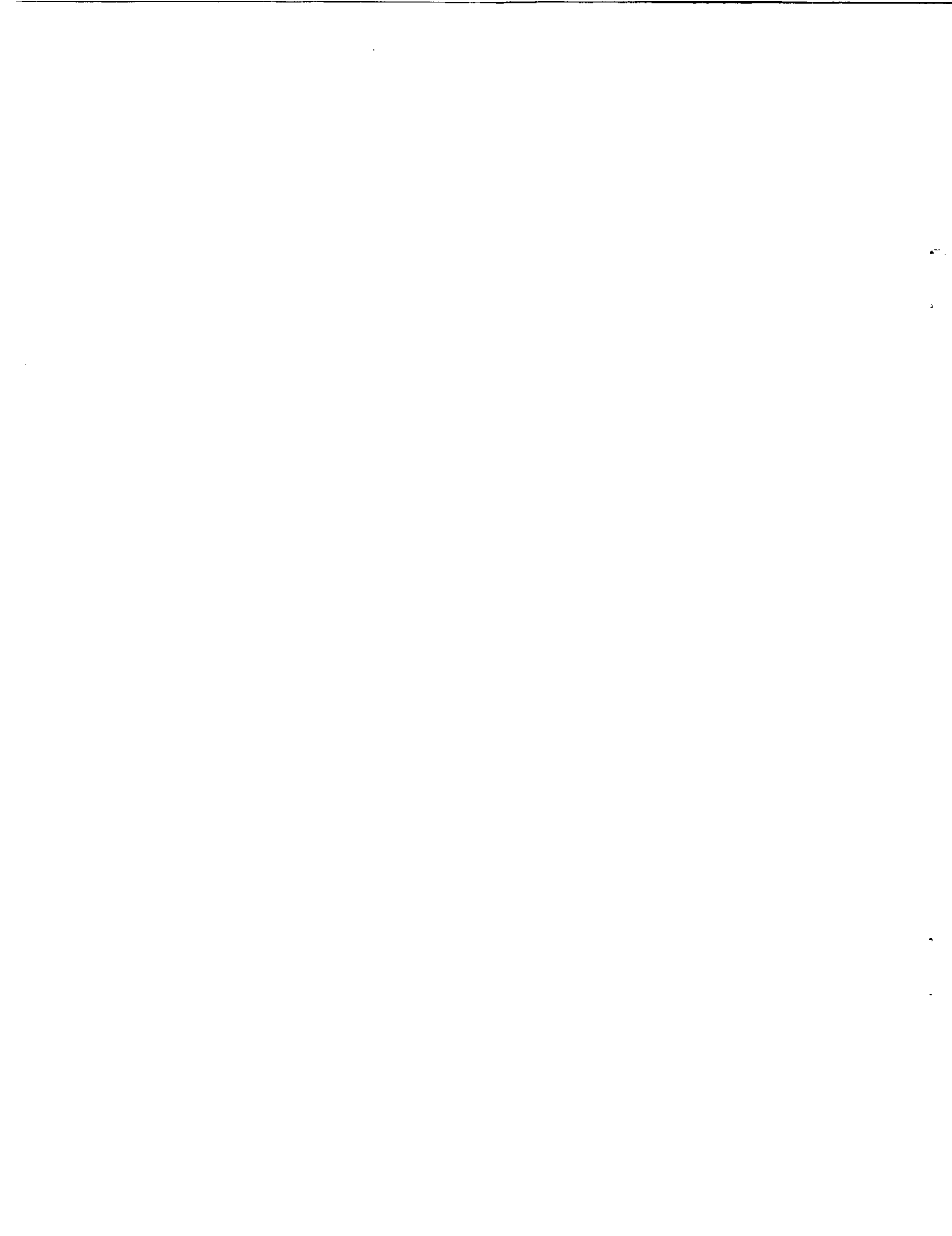
N93-16596

Unclass

G3  
01/02 0139889

Prepared for the  
Ninth Symposium on Turbulence Shear Flows  
Kyoto, Japan, August 10 -18, 1993





# A REALIZABLE REYNOLDS STRESS ALGEBRAIC EQUATION MODEL

Tsan-Hsing Shih and Jiang Zhu  
Institute for Computational Mechanics in Propulsion  
and Center for Modeling of Turbulence and Transition  
NASA Lewis Research Center  
Cleveland, Ohio 44135

John L. Lumley  
Cornell University, Ithaca, New York 14853

## Abstract

The invariance theory in continuum mechanics is applied to analyze Reynolds stresses in high Reynolds number turbulent flows. The analysis leads to a turbulent constitutive relation that relates the Reynolds stresses to the mean velocity gradients in a more general form in which the classical isotropic eddy viscosity model is just the linear approximation of the general form. On the basis of realizability analysis, a set of model coefficients are obtained which are functions of the time scale ratios of the turbulence to the mean strain rate and the mean rotation rate. These coefficients will ensure the positivity of each component of the turbulent kinetic energy — realizability that most existing turbulence models fail to satisfy. Separated flows over backward-facing step configurations are taken as applications. The calculations are performed with a conservative finite-volume method. Grid-independent and numerical diffusion-free solutions are obtained by using differencing schemes of second-order accuracy on sufficiently fine grids. The calculated results are compared in detail with the experimental data for both mean and turbulent quantities. The comparison shows that the present proposal significantly improves the predictive capability of  $K-\epsilon$  based two equation models. In addition, the proposed model is able to simulate rotational homogeneous shear flows with large rotation rates which all conventional eddy viscosity models fail to simulate.

## 1. Introduction

Numerical simulation of turbulence is a bottleneck in the development of computational fluid dynamics (CFD). The approach of direct numerical simulation (DNS) without any turbulence models is restricted to simple and low Reynolds number flows within the capabilities of current computers. A compromise to DNS is the large-eddy simulation (LES) approach in which the large scales of turbulence are directly computed and the small scales are modeled. LES, though applicable for high Reynolds number turbulence, is usually very expensive and has serious problems with boundary conditions. Some of these difficulties also exist in DNS. Therefore, most practical calculations at the present time are based on averaged Navier-Stokes equations with the aid of turbulence modeling.

In turbulence modeling, unknown turbulent correlations are expressed in terms of determinable flow quantities with the aid of empirical information. According to the way the Reynolds stresses (the second-order moment correlations) are treated, turbulence models may be divided into two groups: the Reynolds stress algebraic equation models and the Reynolds stress transport equation models. The former group includes the zero-, one- and two-equation models (Rodi, 1980) in which the Reynolds stresses are algebraically related to the mean flow field. The eddy viscosity  $K-\epsilon$  two-equation model (Launder and Spalding, 1974) in this group is one of the most popular turbulence models used today in practical flow calculations. In the latter group, often called second-order closure models, the Reynolds stresses are determined by their own dynamical transport equations. Second-order closures are attractive because they can simulate the transport of the individual Reynolds stresses; however, it is difficult to consistently model all the higher-order turbulent correlations appearing in these second moment dynamical equations. Inappropriate modeling of higher order correlations (often due to lack of information about their underlying mechanism) could result in a serious inaccuracy and unphysical results.

In the standard  $K-\epsilon$  model, all the model coefficients are constant and are determined from a set of experiments for simple flows under equilibrium or isotropic turbulence conditions (Rodi, 1980). Numerical experience over the last two decades has shown that this set of constants has a broad applicability, but this by no means signifies that they are universal. Rodi (1980) found that the  $K-\epsilon$  model's ability to predict weak shear flows can be significantly improved by using  $C_\mu$  as a function of the average ratio of  $P/\epsilon$  ( $P$  is the production of the turbulent kinetic energy) instead of a constant. Leschziner and Rodi (1981) proposed a function for  $C_\mu$  which takes into account the effect of streamline curvature and obtained improved results in the calculation of annular and twin parallel jets. Recently, Yakhot and co-workers have

developed a version of the  $K-\epsilon$  model using renormalization group (RNG) methods. Their model is of the same form as the standard  $K-\epsilon$  model, but all the model coefficients take different constant values. In the latest version of the RNG based  $K-\epsilon$  model (Speziale and Thangam, 1992), the coefficient  $C_1$ , related to the production of dissipation term, is set to be a function of  $\eta$ , where  $\eta$  is the time scale ratio of the turbulent to mean strain rate. In applying this model to a separated flow over a backward-facing step, experimentally studied by Kim *et al.* (1978), Speziale and Thangam obtained a good prediction of the reattachment length which is an important parameter often used to assess the overall accuracy of calculations.

The standard  $K-\epsilon$  model (including the RNG based one), like many others in the algebraic equation model group, uses Boussinesq's isotropic eddy-viscosity concept which assumes that the Reynolds stresses are proportional to the mean velocity gradients. The concept usually does well for the shear stresses in two-dimensional mean flows of the boundary-layer type, but not well for the normal stresses due to the erroneous isotropic nature of the concept. This suggests that linear dependence on the mean velocity gradients is insufficient and that a more general relation is needed for more complex flows. In fact, by eliminating the convection and diffusion terms in the modeled transport equations for the Reynolds stresses, Rodi (1980) developed an algebraic stress model (ASM) in which the Reynolds stresses are calculated by algebraic expressions. Owing to its anisotropic nature, the model does perform better than the isotropic  $K-\epsilon$  model for certain flows; a well known example is fully-developed flow in non-circular ducts where ASM is capable of generating turbulence-driven secondary motions while the isotropic eddy viscosity  $K-\epsilon$  model is not. However, ASM does not appear in a tensorial invariant form, which may limit its generality. In addition, inappropriate modeling of higher order correlations, such as pressure-strain correlations, will also cause deficiencies of the second-order closure based ASM. Moreover, special care needs to be taken to prevent the turbulent normal stresses from becoming negative (Huang and Leschziner, 1985), and the numerical implementation of ASM may even be more complicated than that of its parent second-order closure model, especially in general three dimensional flows. Recently, this numerical difficulties of ASM was first nicely resolved by Taulbee (1992).

There are other approaches to developing Reynolds stress algebraic equation models. For example, Yoshizawa (1984) derived a relation for the turbulent stresses using a two-scale direct interaction approximation. It contains both linear and quadratic terms of the mean velocity gradients. A similar relation was also derived recently by Rubinstein and Barton (1990) using Yokhot and Orszag's RNG method. An interesting point in these two methods is that the values of the model coefficients can all

be determined analytically. Speziale (1987) proposed a different expression, based on the principle of material frame-indifference, which contains the Oldroyd derivative of the mean strain rates. However, the principle of material frame-indifference is only valid in the limit of two-dimensional incompressible turbulence, hence it is not an appropriate constraint for general turbulent flows. In addition, these non-linear models are not fully realizable and have not been extensively tested.

The purpose of the present study is to develop a general and realizable Reynolds stress algebraic equation model with the method of rational mechanics. As usual, we assume that the Reynolds stresses depend on the mean velocity gradients, the turbulent velocity and length scales, then a constitutive relation for the Reynolds stresses is derived by using the invariance theory. The final form is truncated up to tensorial quadratic terms of the mean velocity gradients. Using the realizability conditions, the coefficients in the obtained relation are found to be at least functions of the time scale ratio of the turbulence to the mean strain rate. In general, they are also functions of the time scale ratio of the turbulence to the mean rotation rate.

The model validation is made on the basis of applications to the rotational homogeneous shear flows simulated by Bardina *et al.* (1983) and the two backward-facing step flows experimentally studied by Driver and Seegmiller (1985) and Kim *et al.* (1978). The latter type of flows has served as a benchmark in validating turbulence models for complex flows. Calculations are carried out with a conservative finite-volume method, and a second-order accurate and bounded differencing scheme, together with sufficiently fine grids, is used to ensure that the solution is both grid-independent and free from numerical diffusion. The calculated results are compared in detail with experimental data as well as with those obtained using standard K- $\epsilon$  model.

## 2. Modeling of Reynolds Stresses

Incompressible turbulent flows are governed by the following Reynolds averaged continuity and Navier-Stokes equations:

$$U_{i,i} = 0 \tag{1}$$

$$U_{i,t} + (U_j U_i - \nu U_{i,j} + \overline{u_i u_j})_{,j} = -\frac{P_{,i}}{\rho} \tag{2}$$

where  $U_i$  are the mean velocity components ( $i = 1, 2, 3$ ),  $p$  is the mean pressure,  $\nu$  and  $\rho$  are the fluid kinematic viscosity and density,  $U_{i,t}$  and  $U_{i,j}$  are derivatives of  $U_i$  with respect to time  $t$  and co-ordinate  $x_j$ , respectively.  $\overline{u_i u_j}$  is the turbulent stress tensor which must be modeled.

The oldest and simplest proposal for modeling the turbulent stress is Boussinesq's isotropic eddy-viscosity concept that assumes an analogy between the viscous stresses in laminar flows and the turbulent stresses in turbulent flows. The general form of this concept is

$$\overline{u_i u_j} = \frac{2}{3} K \delta_{ij} - 2\nu_t S_{ij} \quad (3)$$

where  $\nu_t$  is called the eddy-viscosity and  $S_{ij}$  is the mean strain rate defined by

$$S_{ij} = \frac{1}{2}(U_{i,j} + U_{j,i}) \quad (4)$$

Equation (3) constitutes a common basis for most turbulence models that are extensively used today.

## 2.1 Constitutive relation

Does a general constitutive relation exist for turbulent correlations? Lumley (1970) discussed this problem and found that such relations exist only under the situation in which the length and time scales of turbulence are much smaller than those in the mean flow field so that the effect of initial and boundary conditions on the turbulence is not significant far from the wall. In other situations such as rapidly developing mean flows or in the vicinity of walls, it is questionable whether there exists such a constitutive relation for any turbulent correlation; however, from practical point of view, we can formally derive a "constitutive" relation for any turbulent correlation to solve the closure problem. The validity of such a formally derived relation needs, of course, to be verified with the aid of experiments.

A turbulent constitutive relation, if it exists, is always of functional form. From a modeling point of view and for convenience of application, we neglect the time memory effects in the relation and consider the relationship at the present time as the first order approximation in the time expansion of the functional form. Therefore, we assume that the turbulent stress  $\overline{u_i u_j}$  is a function of the mean deformation tensor  $U_{i,j}$ , the velocity and length scales of turbulence characterized by the turbulent kinetic energy  $K$  and its dissipation rate  $\epsilon$ , i.e.,

$$\overline{u_i u_j} = F_{ij}(U_{i,j}, K, \epsilon) \quad (5)$$

Note that the molecular viscosity  $\nu$  is not included because we restrict our attention here only to high Reynolds number turbulent flows.

The arguments of equation ( 5) contain ten quantities bearing two dimensions. According to the  $\pi$  theorem of dimensional analysis, they may be grouped into eight independent non-dimensional quantities:

$$V_{i,j} = \frac{K}{\epsilon} U_{i,j} \quad (6)$$

By normalizing the turbulent stress as

$$\overline{v_i v_j} = \frac{\overline{u_i u_j}}{2K} \quad (7)$$

equation ( 5) can be written as

$$\overline{v_i v_j} = F_{ij}(V_{i,j}) \quad (8)$$

The form of the tensor valued isotropic function  $F_{ij}$  can be determined by using invariance theory (Lumley, 1978). The basic principle is that an invariant can only be a function of other invariants. In determining a set of independent invariants, we have shown in Appendices A and B (also see Shih, 1992) that only 18 independent tensors can be formed with the tensor  $V_{i,j}$  and its transpose  $V_{j,i}$  according to the generalized Cayley-Hamilton relations. Following Lumley (1978), let  $A_i$  and  $B_j$  be two non-dimensional arbitrary vectors, we may form the following 18 invariants:

$$\begin{aligned} & V_{i,j} A_i B_j, \quad V_{j,i} A_i B_j, \\ & V_{i,k} V_{k,j} A_i B_j, \quad V_{j,k} V_{k,i} A_i B_j, \quad V_{i,k} V_{j,k} A_i B_j, \quad V_{k,i} V_{k,j} A_i B_j, \\ & V_{i,k} V_{j,k}^2 A_i B_j, \quad V_{i,k}^2 V_{j,k} A_i B_j, \quad V_{k,i} V_{k,j}^2 A_i B_j, \quad V_{k,i}^2 V_{k,j} A_i B_j, \\ & V_{i,k} V_{l,k} V_{j,l}^2 A_i B_j, \quad V_{i,k}^2 V_{j,k}^2 A_i B_j, \quad V_{k,i}^2 V_{k,j}^2 A_i B_j, \quad V_{k,i} V_{k,l} V_{j,l}^2 A_i B_j, \\ & V_{k,i} V_{k,l}^2 V_{j,l}^2 A_i B_j, \quad V_{i,k} V_{l,k}^2 V_{l,j}^2 A_i B_j, \\ & V_{i,k} V_{l,k} V_{l,m}^2 V_{j,m}^2 A_i B_j, \quad V_{k,i}^2 V_{k,l}^2 V_{m,l} V_{m,j} A_i B_j \end{aligned} \quad (9)$$

In addition, we have other invariants:

$$\delta_{ij} A_i B_j, \quad A_i A_i, \quad B_i B_i, \quad I, \quad II, \quad III, \quad \dots \quad (10)$$

where  $I, II, III$  are the three invariants of the tensor  $V_{i,j}$ :



$$\begin{aligned}
I &= V_{i,i} \\
II &= \frac{1}{2}(V_{i,i}V_{j,j} - V_{i,j}V_{j,i}) \\
III &= \frac{1}{3!}(V_{i,i}V_{j,j}V_{k,k} - 3V_{i,i}V_{j,k}V_{k,j} + 2V_{i,j}V_{j,k}V_{k,i})
\end{aligned} \tag{11}$$

and ... represents the invariants of other 17 tensors, for example,  $V_{i,j}V_{i,j}$ .

Note that in the above list of invariants we do not include  $V_{i,l}V_{l,k}V_{k,j}A_iB_j$  and higher order terms of this type because they are not independent quantities according to the Cayley-Hamilton theorem:

$$V_{i,l}V_{l,k}V_{k,j} - I \cdot V_{i,k}V_{k,j} + II \cdot V_{i,j} - III\delta_{ij} = 0 \tag{12}$$

Any other possible terms, for example,  $V_{k,i}V_{k,l}V_{m,l}V_{m,j}A_iB_j$ , are also not independent, hence they will not be included.

However, the invariant list can be extended by including any combination of invariants in ( 9) and ( 10), for example,

$$V_{i,j}A_iB_j \cdot f_1(I, II, III, V_{i,j}V_{i,j}, \dots) \tag{13}$$

$$V_{i,k}V_{k,j}A_iB_j \cdot f_2(I, II, III, V_{i,j}V_{i,j}, \dots)$$

where  $f_1$  and  $f_2$  are scalar functions. Of course, these types of invariants are not independent, but they are useful in explaining why the coefficients in the final relation ( 16) are, in general, functions of various invariants of the tensors in question.

As a result, the invariant  $\overline{v_i v_j} A_i B_j$  may be written as a function of the above invariants listed in ( 9), ( 10) and ( 13):

$$\begin{aligned}
\overline{v_i v_j} A_i B_j &= f(V_{i,j}A_iB_j, V_{j,i}A_iB_j, V_{i,k}V_{k,j}A_iB_j, V_{j,k}V_{k,i}A_iB_j, \\
&V_{i,k}V_{j,k}A_iB_j, V_{k,i}V_{k,j}A_iB_j, V_{i,k}V_{j,k}^2A_iB_j, \\
&V_{i,k}^2V_{j,k}A_iB_j, V_{k,i}V_{k,j}^2A_iB_j, V_{k,i}^2V_{k,j}A_iB_j, \\
&V_{i,k}V_{l,k}V_{l,j}^2A_iB_j, V_{i,k}^2V_{j,k}^2A_iB_j, V_{k,i}^2V_{k,j}^2A_iB_j, \\
&V_{k,i}V_{k,l}V_{j,l}^2A_iB_j, V_{k,i}V_{k,l}^2V_{j,l}^2A_iB_j, V_{i,k}V_{l,k}^2V_{l,j}^2A_iB_j, \\
&V_{i,k}V_{l,k}V_{l,m}^2V_{j,m}^2A_iB_j, V_{k,i}^2V_{k,l}^2V_{m,l}V_{m,j}A_iB_j, \\
&\delta_{ij}A_iB_j, A_iA_i, B_iB_i, I, II, III, V_{i,j}V_{i,j}, \dots,
\end{aligned}$$

$$V_{i,j}A_iB_j f_1, \dots) \quad (14)$$

Because  $\overline{v_i v_j} A_i B_j$  is bilinear in arbitrary tensors  $A_i$  and  $B_j$ , we must require that the right hand side of equation ( 14) be also bilinear in  $A_i$  and  $B_j$ . Therefore, equation ( 14) can be reduced to

$$\begin{aligned} \overline{v_i v_j} A_i B_j &= a_1 \delta_{ij} A_i B_j + a_2 V_{i,j} A_i B_j + a_3 V_{j,i} A_i B_j \\ &+ a_4 V_{i,k} V_{k,j} A_i B_j + a_5 V_{j,k} V_{k,i} A_i B_j + a_6 V_{i,k} V_{j,k} A_i B_j \\ &+ a_7 V_{k,i} V_{k,j} A_i B_j + a_8 V_{i,k} V_{j,k}^2 A_i B_j + a_9 V_{i,k}^2 V_{j,k} A_i B_j \\ &+ a_{10} V_{k,i} V_{k,j}^2 A_i B_j + a_{11} V_{k,i}^2 V_{k,j} A_i B_j + a_{12} V_{i,k} V_{l,k} V_{l,j}^2 A_i B_j \\ &+ a_{13} V_{i,k}^2 V_{j,k}^2 A_i B_j + a_{14} V_{k,i}^2 V_{k,j}^2 A_i B_j + a_{15} V_{k,i} V_{k,l} V_{j,l}^2 A_i B_j \\ &+ a_{16} V_{k,i} V_{k,l} V_{j,l}^2 A_i B_j + a_{17} V_{i,k} V_{l,k}^2 V_{l,j}^2 A_i B_j \\ &+ a_{18} V_{i,k} V_{l,k} V_{l,m}^2 V_{j,m}^2 A_i B_j + a_{19} V_{k,i}^2 V_{k,l}^2 V_{m,l} V_{m,j} A_i B_j \end{aligned} \quad (15)$$

Noting that  $A_i$  and  $B_j$  are the arbitrary vectors, we obtain

$$\begin{aligned} \overline{v_i v_j} &= a_1 \delta_{ij} + a_2 V_{i,j} + a_3 V_{j,i} + a_4 V_{i,k} V_{k,j} + a_5 V_{j,k} V_{k,i} + a_6 V_{i,k} V_{j,k} \\ &+ a_7 V_{k,i} V_{k,j} + a_8 V_{i,k} V_{j,k}^2 + a_9 V_{i,k}^2 V_{j,k} + a_{10} V_{k,i} V_{k,j}^2 + a_{11} V_{k,i}^2 V_{k,j} \\ &+ a_{12} V_{i,k} V_{l,k} V_{l,j}^2 + a_{13} V_{i,k}^2 V_{j,k}^2 + a_{14} V_{k,i}^2 V_{k,j}^2 + a_{15} V_{k,i} V_{k,l} V_{j,l}^2 \\ &+ a_{16} V_{k,i} V_{k,l} V_{j,l}^2 + a_{17} V_{i,k} V_{l,k}^2 V_{l,j}^2 + a_{18} V_{i,k} V_{l,k} V_{l,m}^2 V_{j,m}^2 \\ &+ a_{19} V_{k,i}^2 V_{k,l}^2 V_{m,l} V_{m,j} \end{aligned} \quad (16)$$

where the coefficients  $a_1 - a_{19}$  are, due to ( 13), functions of the invariants  $I, II, III, V_{i,j} V_{i,j}, \dots$ , i.e.,

$$a_i = f_i(I, II, III, V_{i,j} V_{i,j}, \dots), \quad i = 1, 2, \dots, 19 \quad (17)$$

Equation ( 16) is a general relationship between two second rank tensors.

The normalized turbulent stresses  $\overline{v_i v_j}$  have two properties

$$\overline{v_i v_j} = \overline{v_j v_i} \quad (18)$$

and

$$\overline{v_i v_i} = 1 \quad (19)$$

Using the properties of ( 18) and ( 19) in equation ( 16), we obtain the following relations:

$$\begin{aligned} a_3 &= a_2, & a_5 &= a_4, & a_9 &= a_8, & a_{11} &= a_{10} \\ a_{12} &= a_{15} = a_{16} = a_{17} = a_{18} = a_{19} = 0 \\ a_1 &= \frac{1}{3}[1 - 2a_2 I - 2a_4 D - (a_6 + a_7)\tilde{D} - 2(a_8 + a_{10})\tilde{\tilde{D}} - (a_{13} + a_{14})\bar{\bar{D}}] \end{aligned} \quad (20)$$

where

$$D = V_{i,j} V_{j,i}, \quad \tilde{D} = V_{i,j} V_{i,j}, \quad \tilde{\tilde{D}} = V_{i,j} V_{i,j}^2, \quad \bar{\bar{D}} = V_{i,j}^2 V_{i,j}^2 \quad (21)$$

After introducing equations ( 20) into ( 16) and converting to the dimensional form, we obtain

$$\begin{aligned} \overline{u_i u_j} &= \frac{2}{3} K \delta_{ij} + 2a_2 \frac{K^2}{\epsilon} (U_{i,j} + U_{j,i} - \frac{2}{3} U_{i,i} \delta_{i,j}) \\ &+ 2a_4 \frac{K^3}{\epsilon^2} (U_{i,k} U_{k,j} + U_{j,k} U_{k,i} - \frac{2}{3} \Pi \delta_{ij}) \\ &+ 2a_6 \frac{K^3}{\epsilon^2} (U_{i,k} U_{j,k} - \frac{1}{3} \tilde{\Pi} \delta_{ij}) \\ &+ 2a_7 \frac{K^3}{\epsilon^2} (U_{k,i} U_{k,j} - \frac{1}{3} \tilde{\Pi} \delta_{ij}) \\ &+ 2a_8 \frac{K^4}{\epsilon^3} (U_{i,k} U_{j,k}^2 + U_{i,k}^2 U_{j,k} - \frac{2}{3} \tilde{\tilde{\Pi}} \delta_{ij}) \\ &+ 2a_{10} \frac{K^4}{\epsilon^3} (U_{k,i} U_{k,j}^2 + U_{k,j} U_{k,i}^2 - \frac{2}{3} \tilde{\tilde{\Pi}} \delta_{ij}) \\ &+ 2a_{13} \frac{K^4}{\epsilon^3} (U_{i,k}^2 U_{j,k}^2 - \frac{1}{3} \bar{\bar{\Pi}} \delta_{ij}) \\ &+ 2a_{14} \frac{K^4}{\epsilon^3} (U_{k,i}^2 U_{k,j}^2 - \frac{1}{3} \bar{\bar{\Pi}} \delta_{ij}) \end{aligned} \quad (22)$$

where

$$\Pi = U_{i,j} U_{j,i}, \quad \tilde{\Pi} = U_{i,j} U_{i,j}, \quad \tilde{\tilde{\Pi}} = U_{i,j} U_{i,j}^2, \quad \bar{\bar{\Pi}} = U_{i,j}^2 U_{i,j}^2 \quad (23)$$

Equation ( 22) is the most general relationship between  $\overline{u_i u_j}$  and  $U_{i,j}$  under the assumption ( 5). Interestingly enough, the first five terms at the right-hand side of equation ( 22) are of the same form as those derived through both the two-scale direct interaction formalism (Yoshizawa, 1984) and the renormalization group method (Rubinstein and Barton, 1990). The fact that the three different theoretical analyses lead to a similar result indicates the rationality of equation ( 22).

In practice, however, a quadratic tensorial form of ( 22) may be sufficient, especially when  $\|U_{i,j}\|K/\epsilon$  is less than unity (which is true if the turbulent time scale is smaller than the time scale of mean flow). Therefore, from now on, we only consider the quadratic form of equation ( 22).

## 2.2 Realizability

Realizability (Schumann, 1977, Lumley, 1978), defined as the requirement of the non-negativity of turbulent normal stresses and Schwarz' inequality between any fluctuating quantities, is a basic physical and mathematical principle that the solution of any turbulence model equation should obey. It also represents a minimal requirement to prevent a turbulence model from producing unphysical results. In the following, this principle will be applied to the constitutive relation ( 22) to derive constraints on its coefficients.

Consider a deformation rate tensor of the form

$$\begin{pmatrix} U_{1,1} & 0 & 0 \\ 0 & U_{2,2} & 0 \\ 0 & 0 & 0 \end{pmatrix} \quad (24)$$

The continuity equation ( 1) gives

$$U_{2,2} = -U_{1,1} \quad (25)$$

and from equation ( 22), the normal stress  $\overline{u_1 u_1}$  can be written as

$$\frac{\overline{u_1 u_1}}{2K} = \frac{1}{3} + 2a_2 \frac{KU_{1,1}}{\epsilon} + \frac{1}{3}(2a_4 + a_6 + a_7) \left( \frac{KU_{1,1}}{\epsilon} \right)^2 \quad (26)$$

Since the time scale ratio of the turbulent to the mean strain rate is defined by

$$\eta = \frac{KS}{\epsilon} \quad (27)$$

where

$$S = (2S_{ij}S_{ij})^{1/2} \quad (28)$$

equation ( 26) can further be written as

$$\frac{\overline{u_1 u_1}}{2K} = \frac{1}{3} + a_2 \eta + \frac{1}{12}(2a_4 + a_6 + a_7)\eta^2 \quad (29)$$

Physically, we know that  $\overline{u_1 u_1}$  will decrease by a vortex stretching with an increase in  $U_{1,1}$ , but  $\overline{u_1 u_1}$  cannot be driven to negative values. Therefore, we must require that

$$\frac{\overline{u_1 u_1}}{2K} > 0, \quad \text{if } 0 < \eta < \infty \quad (30)$$

$$\frac{\overline{u_1 u_1}}{2K} \rightarrow 0, \quad \text{if } \eta \rightarrow \infty \quad (31)$$

$$\left(\frac{\overline{u_1 u_1}}{2K}\right)_{,\eta} \rightarrow 0, \quad \text{if } \eta \rightarrow \infty \quad (32)$$

These are called the realizability conditions. They can be satisfied in various ways of which the simplest way is perhaps the following:

$$2a_2 = -\frac{2/3}{A_1 + \eta} \quad (33)$$

$$2a_4 = \frac{C_{r1}}{f(\eta)} \quad (34)$$

$$2a_6 = \frac{C_{r2}}{f(\eta)} \quad (35)$$

$$2a_7 = \frac{C_{r3}}{f(\eta)} \quad (36)$$

where  $f(\eta)$  is in general a polynomial of  $\eta$  of order higher than 2. We take its simplest form as

$$f(\eta) = A_2 + \eta^3 \quad (37)$$

$A_1, A_2, C_{r1}, C_{r2}$  and  $C_{r3}$  are adjustable constants, but they must satisfy

$$\begin{aligned} A_1 > 0, \quad A_2 > 0, \\ 2C_{r1} + C_{r2} + C_{r3} > 0 \end{aligned} \quad (38)$$

Similar analysis on  $\overline{u_2 u_2}$  and  $\overline{u_3 u_3}$  also leads to equations ( 33) to ( 38). It should be mentioned that equations ( 33) to ( 38) also hold for a three-dimensional pure strain rate tensor

$$\begin{pmatrix} U_{1,1} & 0 & 0 \\ 0 & U_{2,2} & 0 \\ 0 & 0 & U_{3,3} \end{pmatrix} \quad (39)$$

and that any deformation rate tensor can be written in the form of ( 39) in the principal axes of deformation rate tensor.

It can be seen from the above analysis that realizability cannot be fully satisfied if the model coefficients are taken as constant, such as those in the standard K- $\epsilon$  model and in the recent anisotropic models of Speziale (1987), Yoshizawa (1984) and Rubinstein and Barton (1990). In fact, these models satisfy realizability only in the weak sense, that is, they only ensure the positivity of the sum of the normal Reynolds stresses.

Further constraints on the model coefficients can be obtained by considering the deformation rate tensor

$$\begin{pmatrix} 0 & U_{1,2} & 0 \\ 0 & 0 & 0 \\ 0 & 0 & 0 \end{pmatrix} \quad (40)$$

which corresponds to a fully-developed channel flow. In this case, we have

$$\begin{aligned} \overline{u_1 u_1} &= \frac{2}{3}K + \frac{\eta^2 K}{3(A_2 + \eta^3)}(2C_{\tau_2} - C_{\tau_3}) \\ \overline{u_2 u_2} &= \frac{2}{3}K + \frac{\eta^2 K}{3(A_2 + \eta^3)}(2C_{\tau_3} - C_{\tau_2}) \\ \overline{u_3 u_3} &= \frac{2}{3}K - \frac{\eta^2 K}{3(A_2 + \eta^3)}(C_{\tau_2} + C_{\tau_3}) \\ \overline{u_1 u_2} &= -\frac{2\eta K}{3(A_1 + \eta)} \end{aligned} \quad (41)$$

where

$$\eta = \frac{KS}{\epsilon}, \quad S = (2S_{ij}S_{ij})^{1/2} = |U_{1,2}| \quad (42)$$

Experiments indicate that

$$\begin{aligned} \overline{u_1 u_1} &> \frac{2}{3}K \\ \overline{u_2 u_2} &< \frac{2}{3}K \end{aligned} \quad (43)$$

which requires, from equation ( 41), that

$$C_{\tau 2} > 2C_{\tau 3} \quad (44)$$

### 2.3 Rotation effect

The parameter  $\eta$  represents the effect of the mean strain rate, and the effect of the mean rotation rate can be represented by  $\xi$ :

$$\xi = \frac{K\Omega}{\epsilon}, \quad \Omega = (2\Omega_{ij}^* \Omega_{ij}^*)^{1/2}, \quad \Omega_{ij}^* = (U_{i,j} - U_{j,i})/2 + 4\epsilon_{mji}\omega_m \quad (45)$$

where  $\omega_m$  represents the rotation of the frame.

In the present study, we find that it is sufficient to simply include the parameter  $\xi$  only in the coefficient  $a_2$ , i.e.,

$$2a_2 = -\frac{2/3}{A_1 + \eta + \alpha\xi} \quad (46)$$

while keeping the other coefficients the same. The dependance of the coefficients on  $\eta$  and  $\xi$  can be easily justified by equation ( 17).

### 2.4 Realizable algebraic equation model

By introducing equation ( 33)-( 37) into equation ( 22), we obtain

$$\begin{aligned} \overline{u_i u_j} &= \frac{2}{3}K\delta_{ij} - \nu_t(U_{i,j} + U_{j,i}) \\ &+ \frac{C_{\tau 1}}{A_2 + \eta^3} \frac{K^3}{\epsilon^2} (U_{i,k}U_{k,j} + U_{j,k}U_{k,i} - \frac{2}{3}\Pi\delta_{ij}) \\ &+ \frac{C_{\tau 2}}{A_2 + \eta^3} \frac{K^3}{\epsilon^2} (U_{i,k}U_{j,k} - \frac{1}{3}\tilde{\Pi}\delta_{ij}) \\ &+ \frac{C_{\tau 3}}{A_2 + \eta^3} \frac{K^3}{\epsilon^2} (U_{k,i}U_{k,j} - \frac{1}{3}\tilde{\Pi}\delta_{ij}) \end{aligned} \quad (47)$$

Two quantities, the turbulent kinetic energy  $K$  and its dissipation rate  $\epsilon$ , remain to be determined in equation ( 47). To this end, the two transport equations in the standard  $K$ - $\epsilon$  model are used which read:

$$K_{,t} + [U_j K - (\nu + \frac{\nu_t}{\sigma_K})K_{,j}]_{,j} = P - \epsilon \quad (48)$$

$$\epsilon_{,t} + [U_j \epsilon - (\nu + \frac{\nu_t}{\sigma_\epsilon})\epsilon_{,j}]_{,j} = C_1 \frac{\epsilon}{K} P - C_2 \frac{\epsilon^2}{K} \quad (49)$$

where

$$\nu_t = C_\mu \frac{K^2}{\epsilon}, \quad C_\mu = \frac{2/3}{A_1 + \eta + \alpha\xi} \quad (50)$$

$$P = -\overline{u_i u_j} U_{i,j} \quad (51)$$

The coefficients  $C_1, C_2, \sigma_K$  and  $\sigma_\epsilon$  assume their standard values:

$$C_1 = 1.44, \quad C_2 = 1.92, \quad \sigma_K = 1, \quad \sigma_\epsilon = 1.3 \quad (52)$$

and the additional coefficients assume:

$$C_{\tau_1} = -4, \quad C_{\tau_2} = 13, \quad C_{\tau_3} = -2, \quad A_1 = 1.25, \quad \alpha = 0.9, \quad A_2 = 1000. \quad (53)$$

These values have been found to work well for both test cases considered in this work.

### 3. Rotating Homogeneous Shear Flow

The present model is able to mimic the effect of the mean rotation rate on the turbulence. A test case is the rotating homogeneous shear flow which was studied by Bardina *et al.* (1983) using the LES method. Figure 1 is the configuration of the flow being tested. Figures 2(a - c) show the evolution of the turbulent kinetic energy  $K/K_0$  with the nondimensional time,  $St$ , at the rotation rates of  $\Omega/S = 0, 0.5, -0.5$  respectively, where  $K_0$  is the initial turbulent kinetic energy,  $S$  is the mean strain rate and  $\Omega$  is the rotation rate of the reference frame. The calculations were performed with a fourth order Runge-Kutta scheme. The initial condition corresponding to the isotropic turbulence used in LES with  $\epsilon_0/(SK_0) = 0.296$  was adopted for all the three cases. The results from both the present model and the standard K- $\epsilon$  model (hereafter referred to as s-K- $\epsilon$ ) are compared with LES results in figures 2(a - c). It can be seen that at  $\Omega/S = 0$  the present model cannot predict the initial nonequilibrium development of turbulent kinetic energy very well starting from an isotropic turbulence. However, it does catch up with the later "equilibrium" development and performs much better than the s-K- $\epsilon$  model which highly overpredicts the data. Figures 2(b) and 2(c) show the ability of the present model to simulate the effect of the large rotation rate on turbulence. Note that the s-K- $\epsilon$  model gives the same results as for the no rotation case because it cannot account for the effect of rotation on the evolution of turbulence.



## 4. Backward-Facing Step Flows

### 4.1 Numerical procedure

For computational convenience, the non-dimensional form of the governing equations is solved, in which

$$\begin{aligned} \langle x_i \rangle &= \frac{x_i}{L_{ref}}, & \langle U_i \rangle &= \frac{U_i}{U_{ref}}, & \langle p \rangle &= \frac{p}{\rho U_{ref}^2}, \\ \langle K \rangle &= \frac{K}{U_{ref}^2}, & \langle \epsilon \rangle &= \frac{\epsilon L_{ref}}{U_{ref}^3}, & \langle \nu_t \rangle &= \frac{\nu_t}{U_{ref} L_{ref}} \end{aligned} \quad (54)$$

where  $\langle \rangle$  refers to a non-dimensional quantity, and  $L_{ref}$ , and  $U_{ref}$  are the reference length and velocity, respectively. Accordingly, the flow Reynolds number is defined by

$$Re = \frac{L_{ref} U_{ref}}{\nu} \quad (55)$$

Hereafter, all the quantities will be of the non-dimensional form so that  $\langle \rangle$  will be dropped for simplicity.

In the steady-state and two dimensional cases ( $x_1 = x, x_2 = y$ ), the transport equations ( 1), ( 2), ( 48) and ( 49) can be written in the following general form

$$[U\phi - (\frac{1}{Re} + \frac{\nu_t}{\sigma_\phi})\phi_{,x}]_{,x} + [V\phi - (\frac{1}{Re} + \frac{\nu_t}{\sigma_\phi})\phi_{,y}]_{,y} = S_\phi \quad (56)$$

where  $\phi$  stands for 1,  $U(= U_1)$ ,  $V(= U_2)$ ,  $K$  and  $\epsilon$ . For the momentum equations, the source term  $S_\phi$  includes the cross-derivative diffusion and quadratic velocity gradient terms arising from equation ( 47). It can be seen that the non-dimensional equations are all of the same form as their dimensional counterparts, except that the kinematic molecular viscosity  $\nu$  is replaced by  $1/Re$ .

The numerical method used to solve the system of equations ( 56) is a finite-volume procedure. It uses a non-staggered grid with all the dependent variables being stored at the geometric center of each control volume (Figure 3). The momentum interpolation procedure of Rhie and Chow (1983) is used to avoid spurious oscillations usually associated with the non-staggered grid, and the pressure-velocity coupling is handled with the SIMPLEC algorithm (Van Doormal and Raithby, 1984). To ensure both accuracy and stability of numerical solution, the convection terms are approximated by a second-order accurate and bounded differencing scheme (Zhu, 1991a), and all the other terms by the conventional central differencing scheme. As

a result, the discretized counterpart of equation ( 56) can be cast into the following linearized form

$$\sum_l A_l \phi_C = A_l \phi_l + S_C \quad (57)$$

where the coefficients  $A_l$  ( $l = W, E, S, N$ ), which relate the principal unknown  $\phi_C$  to its neighbours  $\phi_l$  (Figure 3), result from the discretization of the left-hand side terms of equation ( 56). The convection scheme used ensures that  $A_l \geq 0$  so that the resulting coefficient matrix is always diagonally dominant. The strongly implicit procedure of Stone (1968) is used to solve the system of algebraic equations. The iterative solution process is considered converged when the maximum normalized residue of all the dependent variables is less than  $10^{-4}$ . The details of the present numerical procedure are given in Rodi *et al.* (1989) and Zhu (1991b).

## 4.2 Numerical results

The present model is then applied to the two backward-facing step flows experimentally studied by Kim, Kline and Johnston (1978) and Driver and Seegmiller (1985), from here on referred to as KKJ- and DS-cases, respectively. Figure 4 shows the flow configuration and the Cartesian co-ordinate system used. Table 1 gives the flow parameters for both cases; here the experimental reference free-stream velocity  $U_{ref}$  and step height  $H_s$  are taken as the reference quantities for non-dimensionalization.

Table 1. Flow parameters

case	$Re$	$\delta$	$L_s$	$L_e$	$H_s$	$H_d$	$U_{ref}$
DS	37423	1.5	10	40	1	8	1
KKJ	44737	0.6	10	40	1	2	1

Three types of boundaries are present, i.e. inlet, outlet and solid wall. At the inlet, the experimental data are available for the streamwise mean velocity  $U$  and the turbulent normal stresses  $\overline{uu}$  and  $\overline{vv}$ .  $K$  is calculated from these  $\overline{uu}$  and  $\overline{vv}$  with the assumption that

$$\overline{ww} = \frac{1}{2}(\overline{uu} + \overline{vv}) \quad (58)$$

and  $\epsilon$  by

$$\epsilon = \frac{C_\mu^{3/4} K^{3/2}}{L}, \quad L = \min(0.41\Delta y, 0.085\delta) \quad (59)$$

where  $\Delta y$  is the distance from the wall and  $\delta$  is the boundary-layer thickness given in Table 1. At the outlet, the streamwise derivatives of the flow variables are set to zero. Influences of both inlet and outlet conditions on the solution are examined by changing the locations  $L_s$  and  $L_e$ , and it has been found that in both cases, the distances given in Table 1 are already sufficiently far away from the region of interest. In the earlier stage of this work, we tested several low Reynolds number  $K-\epsilon$  models including those of Chien (1982), Lam and Bremhorst (1981), Launder and Sharma (1974), Shih and Lumley (1992), and Yang and Shih (1992), but none of them was found to be able to yield satisfactory solutions. Similar findings were also reported in Avva *et al.* (1990), Shuen (1992) and So and Lai (1988). Therefore in this work, we use the standard wall function approach (Launder and Spalding, 1974) to bridge the viscous sublayer near the wall.

Two sets of non-uniform computational grids are used to examine the grid dependence of the solution; they contain  $110 \times 52$  (coarse) and  $199 \times 91$  (fine) points for the KKJ-case and  $106 \times 56$  (coarse) and  $201 \times 109$  (fine) points for the DS-case. Figures 5(a) and 5(b) show the friction coefficient  $C_f$  at the bottom wall calculated with the s-K- $\epsilon$  model and the present model; also included in figure 5(a) are the experimental data for the DS-case, but no such data are available for the KKJ-case. It can be seen that the grid refinement does produce some differences for the results of the present model, more noticeable in the KKJ-case, and this is also the case for the s-K- $\epsilon$  results. This indicates that the solutions obtained on the coarse grids are not sufficiently close to the grid-independent stage. Recently, Thangam and Hur (1991) have conducted a highly-resolved calculation for the KKJ-case. They have found that quadrupling a  $166 \times 73$  grid leads to only a minimal improvement. Therefore, the present results on the fine grids can be considered as grid-independent. For the DS-case, the fine grid computations with the s-K- $\epsilon$  and present model required 703 and 805 iterations, and took approximately 7.1 and 8.3 minutes of CPU time on the Cray YMP computer. In the following, only the fine grid results are presented.

The wall friction coefficient  $C_f$  is a parameter that is very sensitive to the near-wall turbulence modeling. It is  $C_f$  that the various low Reynolds number  $K-\epsilon$  models tested predict much worse than those using wall functions. However, the influence of the near-wall turbulence modeling is only restricted in the near-wall regions. It is seen from figure 5(a) that both the s-K- $\epsilon$  and present model largely underpredict the negative peak of  $C_f$ , pointing to limited accuracy of the wall function approach in the recirculation region.

The computed and measured reattachment points are compared in Table 2. They are determined in the calculation from the point where  $C_f$  goes to zero. Also included in Table 2 are the result of Obi *et al.* (1989) obtained with the Reynolds stress model

(RSM) and that of Sindir (1982) with a modified algebraic stress model (ASM). The reattachment point is a critical parameter which has often been used to assess the overall performance of turbulence models as well as numerical procedures. Table 2 clearly demonstrates the significant improvement obtained with the present model. It is important to mention that this improvement is mainly due to the behavior of  $C_\mu$  in the present model, and that the anisotropic behavior of the turbulent stresses only makes a marginal contribution to it.

Table 2. Comparison of reattachment points

case	experiment	s-K- $\epsilon$	present model	RSM	ASM
DS	6.1	4.99	5.82	-	5.66
KKJ	$7 \pm 0.5$	6.35	7.35	6.44	-

Figures 6(a) and 6(b) show the comparison of computed and measured static pressure coefficient  $C_p$  along the bottom wall. In both cases, the s-K- $\epsilon$  is seen to predict premature pressure rises, which is consistent with its underprediction of the reattachment lengths, while the present model captures these pressure rises quite well. The good predictions of  $C_p$  were reported in both works of Obi *et al.* (1989) and Sindir (1982), using the RSM and ASM. The results of the present model are almost comparable to those of the RSM and ASM. Again, the improved predictions of  $C_p$  are mainly attributed to the variation of  $C_\mu$ .

The streamwise mean velocity  $U$  profiles are shown in figures 7(a) and 7(b) at four different cross-sections. Here, the differences between the results of the s-K- $\epsilon$  and present model are not substantial, as compared to other flow variables. The present model predicts reverse flows better than the s-K- $\epsilon$ , but results in somewhat slower recovery in the vicinity of the reattachment point. Interestingly enough, such a slow recovery also exists in the RSM prediction of Obi *et al.* (1989). Further downstream, say at  $x=20$  in figure 7(a), the results of the two models nearly coincide with each other.

Finally, the comparisons of predicted and measured turbulent stresses  $\overline{u^2}$ ,  $\overline{v^2}$  and  $\overline{uv}$  are shown in figures 8 and 9 at various  $x$ -locations. In the KKJ-case, no experimental data for the turbulent stresses are available in the recirculation region, and the reattachment point was found in the experiment to move forward and backward continuously around seven step heights downstream of the step, leaving an uncertainty of  $\pm 0.5$  step height for the reattachment length. This also points to some uncertainty in the measured turbulent quantities in the recovery region. On the other hand, the experimental data in the DS-case should be considered more reliable because of the smaller uncertainty of the reattachment location, indicating a smaller unsteadiness of the flow. As compared with the s-K- $\epsilon$  results in figures

8 and 9, it can be seen that the anisotropic terms increase  $\overline{u^2}$  while decreasing  $\overline{v^2}$ , leading to significant improvements in both  $\overline{u^2}$  and  $\overline{v^2}$  results. On the other hand, the anisotropic terms have little impact on the turbulent shear stress  $\overline{uv}$ . These behaviours are clearly reflected in equations (41) which also hold qualitatively for the flows considered here. The improvement obtained by the present model in figure 8 for  $\overline{uv}$  is due to the reduction in  $C_\mu$ .

## 5. Conclusions

A constitutive relation for the turbulent stresses has been derived by using invariance theory. The relation is valid only for turbulent flows at high Reynolds numbers because the influence of the molecular viscosity has not been taken into account in the analysis. Being a second rank tensor, the general form of the turbulent stress can be expressed as a series, in terms of the mean velocity gradients, of order up to 4, while the classical eddy-viscosity representation constitutes only a first-order approximation. For practical calculations, it may suffice to use the quadratic approximation. The model coefficients are functions of the time scale ratios  $\eta$  and  $\xi$ , which ensure the positiveness of the turbulent normal stresses - a realizability condition that most existing turbulence models are unable to satisfy. The present model has been applied to calculate the two different flows: rotating homogeneous shear flows and backward-facing step flows. The calculated results show that all flow variables are sensitive to the variation of  $C_\mu$ , and that only the turbulent normal stresses are sensitive to the terms containing nonlinear mean velocity gradients. The values of the model coefficients given in this paper seem quite appropriate for both the test cases, but the value of  $C_{\tau_1}$  related to the cross-derivative quadratic terms has little impact on the flows considered. This indicates that  $C_{\tau_1}$  may be further calibrated against other flows. The computed results have been compared in detail with the LES data for rotating homogeneous shear flows and the experimental data for backward-facing step flows. The comparisons show that the present model does provide significant improvement over the standard K- $\epsilon$  model, and this improvement is achieved at an insignificant penalty to the computational efficiency and algorithmic simplicity of the latter. The present model can also be expected to work well for simple inhomogeneous shear flows, as evidenced by its improved prediction in the region far downstream of the reattachment point where the flow tends to be of simple parabolic nature.

## Acknowledgements

The authors are grateful to Dr. Aamir Shabbir for his calculations of the rotating homogeneous shear flows and for many helpful suggestions and discussions. The contribution of J.L. Lumley was supported in part by Contract No. AFOSR 89-0226, jointly funded by the U.S. Airforce Office of Scientific Research (Control and Aerospace Programs), and the U.S. Office of Naval Research, and in part by Grant No. F49620-92-J-0038, funded by the U.S. Airforce Office of Scientific Research (Aerospace Program).

## References

1. R.K. Avva, C.E. Smith and A.K. Singhal, 1990, "Comparative study of high and low Reynolds number versions of K- $\epsilon$  models", AIAA paper 90-0246.
2. J. Bardina, J.H. Ferziger and W.C. Reynolds, 1983, "Improved turbulence models based on large-eddy simulation of homogeneous incompressible turbulent flows." Rept. No.TF-19, Stanford University, Stanford, Ca.
3. K.Y. Chien, 1982, "Predictions of channel and boundary-layer flows with a low-Reynolds-number turbulence model", *AIAA J.*, Vol.20, pp.33-38.
4. D.M. Driver and H.L. Seegmiller, 1985, "Features of a reattaching turbulent shear layer in divergent channel flow", *AIAA J.*, Vol.23, pp.163-171.
5. P.G. Huang and M.A. Leschziner, 1985, "Stabilization of recirculating-flow computations performed with second moment closures and third order discretization", *Proceedings of the 5th Symposium on Turbulent Shear Flows*, Cornell University, pp.5.19-5.24.
6. J. Kim, S.J. Kline and J.P. Johnston, 1978, "Investigation of separation and reattachment of a turbulent shear layer: Flow over a backward-facing step", Rept. MD-37, Thermosciences Div., Dept. of Mech. Eng., Stanford University.
7. C.K.G. Lam and K. Bremhorst, 1981, "A modified form of K- $\epsilon$  model for predicting wall turbulence", *J. Fluids Eng.*, Vol.103, pp.456-460.

8. B.E. Launder and B.I. Sharma, 1974, "Application of the energy-dissipation model of turbulence to the calculation of a flow near a spinning disk", *Letters in Heat and Mass transfer* Vol.1, pp.131-138.
9. B.E. Launder and D.B. Spalding, 1974, "The numerical computation of turbulent flows", *Comput. Meths. App. Mech. Eng.*, Vol.3, pp.269-289.
10. M.A. Leschziner and W. Rodi, 1981, "Calculation of annular and twin parallel jets using various discretization schemes and turbulence model variations", *J. Fluids Eng.*, Vol.103, pp.352-360.
11. J.L. Lumley, 1970, "Toward a turbulent constitutive relation." *J. Fluid Mech.*, Vol.41, pp.413-434.
12. J.L. Lumley, 1978, "Computational modeling of turbulent flows", *Adv. Appl. Mech.*, Vol.18, pp.124-176.
13. S. Obi, M. Peric and G. Scheuerer, 1989, "A finite-volume calculation procedure for turbulent flows with second-order closure and co-located variable arrangement", Report. LSTM 276/N/89, Lehrstuhl für Strömungsmechanik, Universität Erlangen-Nürnberg.
14. R.S. Rivlin, 1955, "Further remarks on the stress deformation relations for isotropic materials", *J. Arch. Ratl. Mech. Anal.*, Vol.4, pp.681-702.
15. C.M. Rhie and W.L. Chow, 1983, "A numerical study of the turbulent flow past an isolated airfoil with trailing edge separation", *AIAA J.*, Vol.21, pp.1525-1532.
16. W. Rodi, 1980, "Turbulence models and their application in hydraulics - A state of the art review", Book Publication of the International Association for Hydraulic Research, Delft, the Netherlands.
17. W. Rodi, S. Majumdar and B. Schönung, 1989, "Finite-volume method for two dimensional incompressible flows with complex boundaries", *Comput. Meths. App. Mech. Eng.*, Vol.75, pp.369-392.
18. R. Rubinstein and J.M. Barton, 1990, "Nonlinear Reynolds stress models and the renormalization group", *Phys. Fluids A* 2, pp.1472-1476.
19. U. Schumann, 1977, "Realizability of Reynolds stress turbulence models", *Phys. Fluids*, Vol.20, pp.721-725.

20. T.H. Shih, 1992, "Remarks on turbulent constitutive relations." to appear in NASA TM.
21. T.H. Shih and J.L. Lumley, 1992, "Kolmogorov behavior of near-wall turbulence and its application in turbulence modeling". NASA TM 105663, also in *Int. J. Comput. Fluid Dynamics*, Vol.1.
22. J.S. Shuen, 1992, Private communication.
23. M. Sindir, 1982, "Numerical study of separating and reattaching flows in a backward-facing step geometry", Ph.D. Thesis, University of California at Davis.
24. R.M.C. So and Y.G. Lai, 1988, "Low-Reynolds-number modelling of flows over a backward-facing step", *J. Appl. Math. Phys. (ZAMP)*, Vol.39, pp.13-27.
25. C.G. Speziale, 1987, "On nonlinear K- $\epsilon$  and K- $\epsilon$  models of turbulence", *J. Fluid Mech.*, Vol.178, pp.459-475.
26. C.G. Speziale and S. Thangam, 1992, "Analysis of an RNG based turbulence model for separated flows", NASA CR-189600, ICASE Report. No.92-3.
27. H.L. Stone, 1968, "Iterative solution of implicit approximations of multidimensional partial differential equation", *SIAM J. Num. Anal.*, Vol.5, pp.530-558.
28. D.B. Taulbee, 1992, "An improved algebraic Reynolds stress model and corresponding nonlinear stress model", *Phys. Fluids A*, Vol.4, No.11, pp.2555-2561.
29. S. Thangam and N. Hur, 1991, "A highly-resolved numerical study of turbulent separated flow past a backward-facing step", *Int. J. Eng. Sci.*, Vol.29, pp.607-615.
30. J.P. Van Doormal and G.D. Raithby, 1984, "Enhancements of the SIMPLE method for predicting incompressible fluid flows", *Num. Heat Trans.*, Vol.7, pp.147-163.
31. Z. Yang and T.H. Shih, 1992, "A new time scale based K- $\epsilon$  model for near wall turbulence", NASA TM 105768.
32. A. Yoshizawa, 1984, "Statistical analysis of the derivation of the Reynolds stress from its eddy-viscosity representation", *Phys. Fluids*, Vol.27, pp.1377-1387.
33. J. Zhu, 1991a, "A low diffusive and oscillation-free convection scheme", *Comm. App. Num. Methods.*, Vol.7, pp.225-232.



34. J. Zhu, 1991b, "FAST-2D: A computer program for numerical simulation of two-dimensional incompressible flows with complex boundaries", Rept. No.690, Institute for Hydromechanics, University of Karlsruhe.

# Appendix A

## Generalized Cayley-Hamilton Formulas

Rivlin (1955) showed that there are several generalized Cayley-Hamilton formulas relating matrices (product of several matrices  $A, B, C \dots$ ) of higher extension to matrices of lower extension. Some of them are listed here for latter use.

$$\begin{aligned}
 & ABC + ACB + BCA + BAC + CAB + CBA - A(\text{tr}BC - \text{tr}B \text{tr}C) \\
 & - B(\text{tr}CA - \text{tr}C \text{tr}A) - C(\text{tr}AB - \text{tr}A \text{tr}B) \\
 & - (BC + CA)\text{tr}A - (CA + AC)\text{tr}B - (AB + BA)\text{tr}C \tag{A.1} \\
 & - I(\text{tr}A \text{tr}B \text{tr}C - \text{tr}A \text{tr}BC - \text{tr}B \text{tr}CA \\
 & - \text{tr}C \text{tr}AB + \text{tr}ABC + \text{tr}CBA) = 0
 \end{aligned}$$

Replacing  $C$  with  $A$  and  $B$  in Eq.( A.1), respectively, we obtain

$$\begin{aligned}
 & ABA = -A^2B - BA^2 + A(\text{tr}AB - \text{tr}A \text{tr}B) \\
 & + \frac{1}{2} B(\text{tr}A^2 - \text{tr}A \text{tr}A) + (AB + BA)\text{tr}A + A^2\text{tr}B \tag{A.2} \\
 & + I[\text{tr}A^2B - \text{tr}A \text{tr}AB + \frac{1}{2}\text{tr}B(\text{tr}A \text{tr}A - \text{tr}A^2)]
 \end{aligned}$$

and

$$\begin{aligned}
 & BAB = -B^2A - AB^2 + B(\text{tr}BA - \text{tr}B \text{tr}A) \\
 & + \frac{1}{2} A(\text{tr}B^2 - \text{tr}B \text{tr}A) + (BA + AB)\text{tr}B + B^2\text{tr}A \tag{A.3} \\
 & + I[\text{tr}B^2A - \text{tr}B \text{tr}BA + \frac{1}{2}\text{tr}A(\text{tr}B \text{tr}B - \text{tr}B^2)]
 \end{aligned}$$

which indicate that the matrices  $ABA$  and  $BAB$  of extension 3 can be expressed by polynomials of matrices of extension 2 or less.

Multiplying Eq.( A.2) from the left and the right by  $A$  and Eq.( A.3) by  $B$ , and adding them correspondingly, we obtain following two relations:

$$\begin{aligned} ABA^2 + A^2BA &= ABA \operatorname{tr}A + A^2 \operatorname{tr}AB + A(\operatorname{tr}A^2B - \operatorname{tr}A \operatorname{tr}AB) \\ &- B \operatorname{det}A + I \operatorname{det}A \operatorname{tr}B \end{aligned} \quad (\text{A.4})$$

and

$$\begin{aligned} BAB^2 + B^2AB &= BAB \operatorname{tr}B + B^2 \operatorname{tr}BA + B(\operatorname{tr}B^2A - \operatorname{tr}B \operatorname{tr}BA) \\ &- A \operatorname{det}B + I \operatorname{det}B \operatorname{tr}A \end{aligned} \quad (\text{A.5})$$

Replacing  $B$  with  $B^2$  in Eq.( A.4) and  $A$  with  $A^2$  in Eq.( A.5) give

$$\begin{aligned} AB^2A^2 + A^2B^2A &= AB^2A \operatorname{tr}A + A^2 \operatorname{tr}AB^2 \\ &+ A(\operatorname{tr}A^2B^2 - \operatorname{tr}A \operatorname{tr}AB^2) - B^2 \operatorname{det}A + I \operatorname{det}A \operatorname{tr}B^2 \end{aligned} \quad (\text{A.6})$$

and

$$\begin{aligned} BA^2B^2 + B^2A^2B &= BA^2B \operatorname{tr}B + B^2 \operatorname{tr}BA^2 \\ &+ B(\operatorname{tr}B^2A^2 - \operatorname{tr}B \operatorname{tr}BA^2) - A^2 \operatorname{det}B + I \operatorname{det}B \operatorname{tr}A^2 \end{aligned} \quad (\text{A.7})$$

Replacing  $B$  with  $B^2$  in Eq.( A.2) and  $A$  with  $A^2$  in Eq.( A.3) yield

$$\begin{aligned} AB^2A &= -A^2B^2 - B^2A^2 + A(\operatorname{tr}AB^2 - \operatorname{tr}A \operatorname{tr}B^2) \\ &+ \frac{1}{2} B^2(\operatorname{tr}A^2 - \operatorname{tr}A \operatorname{tr}A) + (AB^2 + B^2A)\operatorname{tr}A + A^2\operatorname{tr}B^2 \\ &+ I[\operatorname{tr}A^2B^2 - \operatorname{tr}A \operatorname{tr}AB^2 + \frac{1}{2}\operatorname{tr}B^2(\operatorname{tr}A \operatorname{tr}A - \operatorname{tr}A^2)] \end{aligned} \quad (\text{A.8})$$

and

$$\begin{aligned} BA^2B &= -B^2A^2 - A^2B^2 + B(\operatorname{tr}BA^2 - \operatorname{tr}B \operatorname{tr}A^2) \\ &+ \frac{1}{2} A^2(\operatorname{tr}B^2 - \operatorname{tr}B \operatorname{tr}A^2) + (BA^2 + A^2B)\operatorname{tr}B + B^2\operatorname{tr}A^2 \\ &+ I[\operatorname{tr}B^2A^2 - \operatorname{tr}B \operatorname{tr}BA^2 + \frac{1}{2}\operatorname{tr}A^2(\operatorname{tr}B \operatorname{tr}B - \operatorname{tr}B^2)] \end{aligned} \quad (\text{A.9})$$

Eqs.( A.8) and ( A.9) indicate that the matrices  $AB^2A$  and  $BA^2B$  of extension 3 can be expressed by polynomials of matrices of extension 2 or less. Therefore, the right hand sides of Eqs.( A.6) and ( A.7) are also polynomials of matrices of extension of 2 or less.

# Appendix B

## Number of Independent Tensors Formed by Two Tensors

Let us show that the number of independent tensors formed with two general tensor  $A$  and  $B$  is 18.

Rivlin (1955) showed that any matrix product in two  $3 \times 3$  matrices may be expressed as a polynomial in these matrices of extension 4 or less. Suppose we have a matrix product  $\Pi$  of extension 5:

$$\Pi = ABA^2B^2A \quad (\text{B.1})$$

This can be written as

$$\Pi = ACA \quad (\text{B.2})$$

where  $C = BA^2B^2$ . From Eq.( A.2),  $\Pi$  may be viewed as a polynomial of matrices in  $A$  and  $C$  of extension 2 or less.  $C$  itself is a matrix in  $A$  and  $B$  of extension 3 so that  $\Pi$  may be expressed by a polynomial in  $A$  and  $B$  of extension 4 or less. Therefore, we only need to consider the possible tensors of extension 4 or less formed by  $A$  and  $B$ .

We may show that there are only two independent tensors of extension 4. The possible tensors of extension 4 are the following 8 tensors:

$$\begin{aligned} &ABA^2B^2, BAB^2A^2, A^2BAB^2, B^2ABA^2, \\ &AB^2A^2B, BA^2B^2A, A^2B^2AB, B^2A^2BA. \end{aligned} \quad (\text{B.3})$$

With Eq.( A.4),  $A^2BAB^2$  can be expressed by  $ABA^2B^2 + \dots$ . Similarly, with Eq.( A.5),  $B^2ABA^2 = -BAB^2A^2 + \dots$ ; with Eq.( A.7),  $AB^2A^2B = -ABA^2B^2 + \dots$ ; with Eq.( A.6),  $BA^2B^2A = -BAB^2A^2 + \dots$ ; with Eqs.( A.5) and ( A.4),  $A^2B^2AB = ABA^2B^2 + \dots$ ; with Eqs.( A.4) and ( A.5),  $B^2A^2BA = BAB^2A^2 + \dots$ ; where  $\dots$  represents a polynomial in  $A$  and  $B$  of extension 3 or less. As a result, only two tensors of extension 4 in Eq.( B.3) are independent, and we select them as

$$ABA^2B^2, \quad BAB^2A^2 \quad (\text{B.4})$$

Now we show that there are only four independent tensors of extension 3. The possible tensors of extension 3 are the following 8 tensors:

$$ABA^2, A^2BA, BAB^2, B^2AB, AB^2A^2, A^2B^2A, BA^2B^2, B^2A^2B. \quad (\text{B.5})$$

Using Eqs.( A.4), ( A.5), ( A.6) and ( A.7), we find that only four of them are independent. Let us select them as

$$ABA^2, BAB^2, AB^2A^2, BA^2B^2. \quad (\text{B.6})$$

Furthermore, there are eight independent tensors of extension 2:

$$AB, BA, AB^2, B^2A, A^2B, BA^2, A^2B^2, B^2A^2 \quad (\text{B.7})$$

and four independent tensors of extension 1:

$$A, A^2, B, B^2. \quad (\text{B.8})$$

Therefore, we have proved that only 18 tensors can be formed independently by two general tensors.

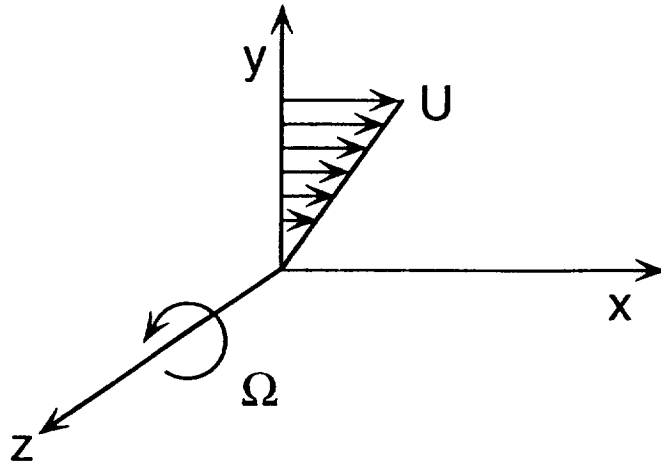


Figure 1. Rotating homogeneous shear flow

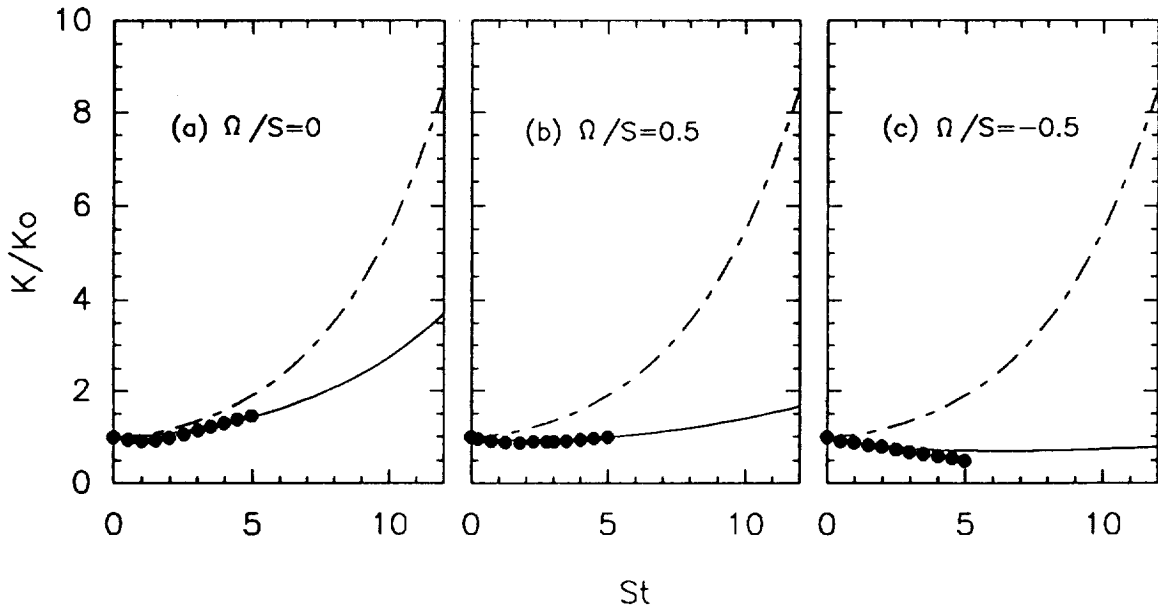


Figure 2. Evolution of turbulent kinetic energy with time.

- - -: s-K- $\epsilon$ ; —: present model; •: LES.

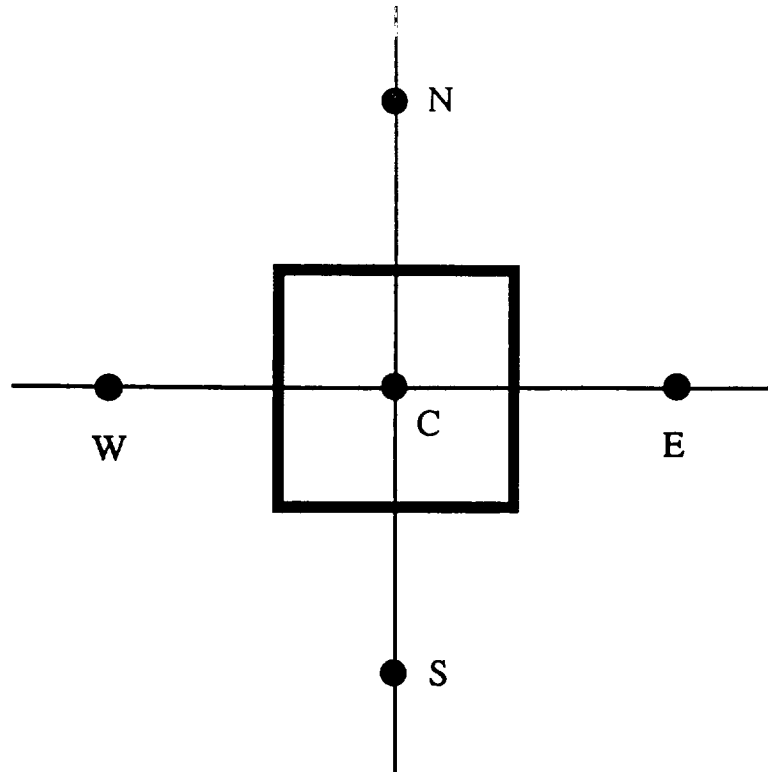


Figure 3. Typical control volume centered at C and related nodes

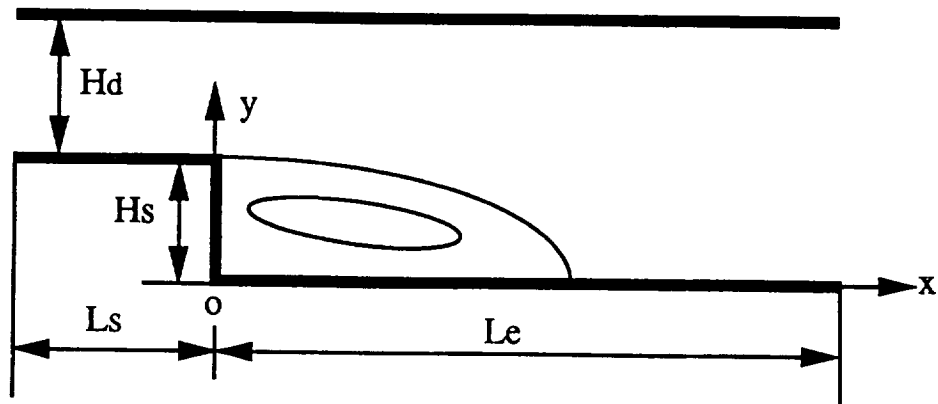


Figure 4. Backward-facing step geometry

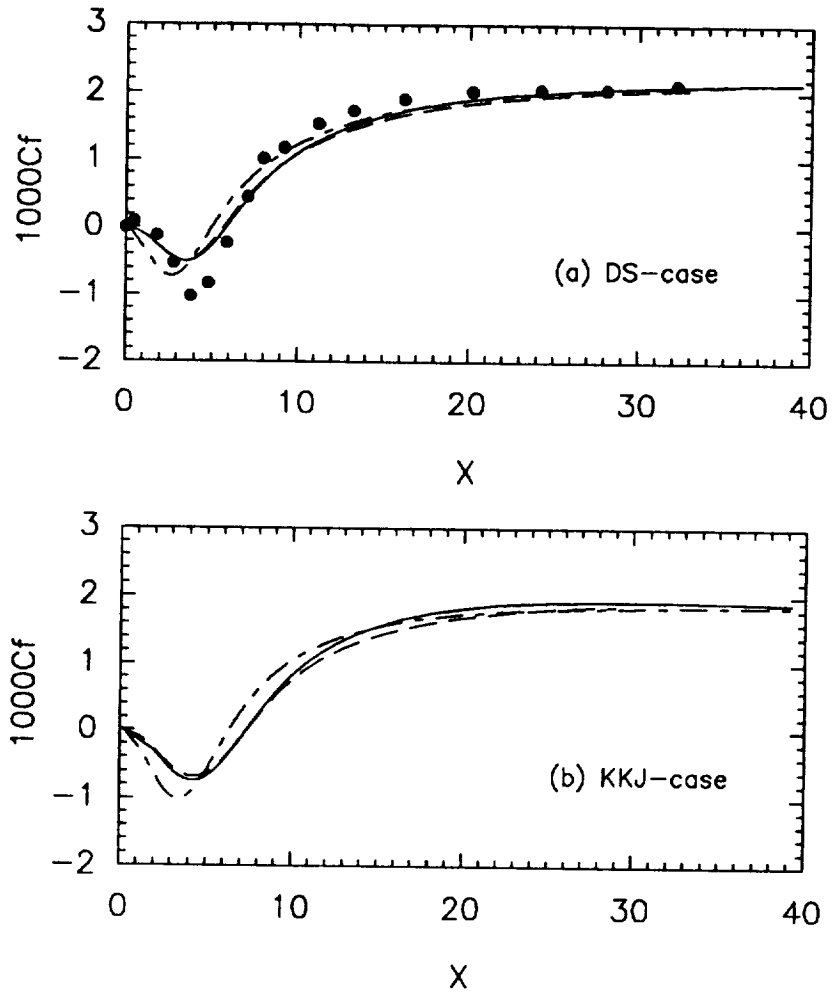


Figure 5. Friction coefficient  $C_f$  along the bottom wall.  
 - - - : s-K- $\epsilon$ , fine grid; — : present model, fine grid;  
 - · - : present model, coarse grid; ● : experiment.



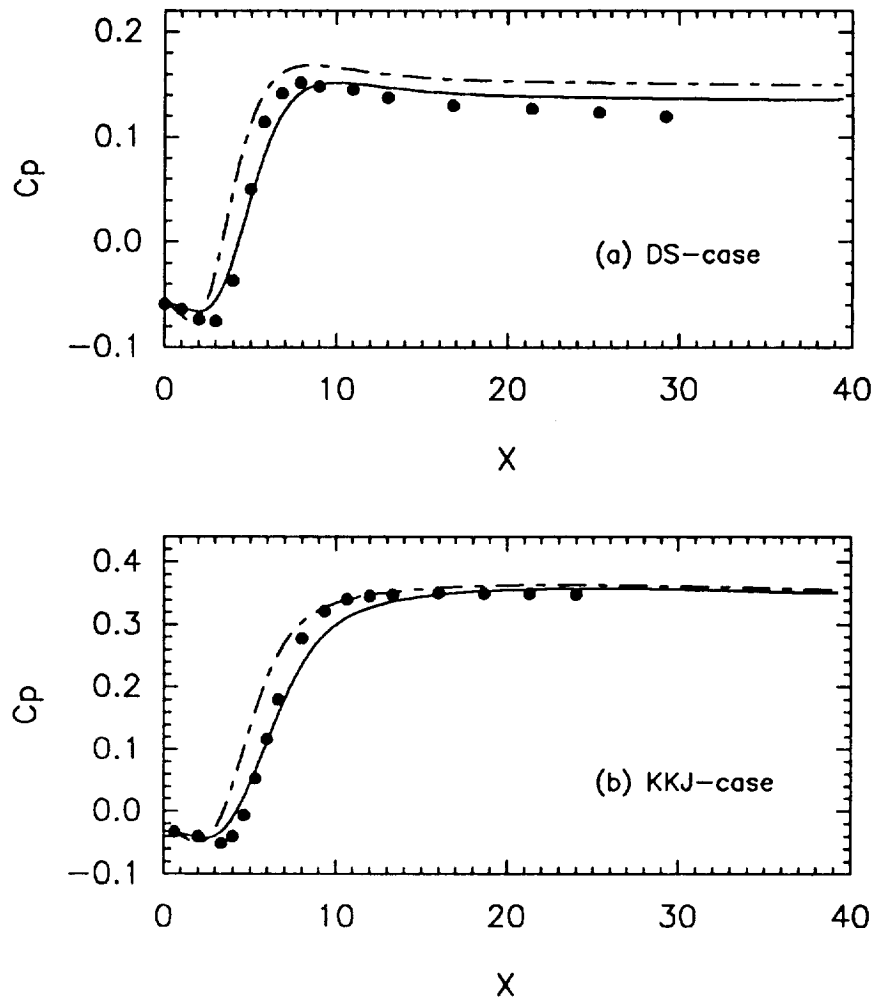


Figure 6. Static pressure coefficient  $C_p$  along the bottom wall.  
 - - -: s-K- $\epsilon$ ; —: present model; •: experiment

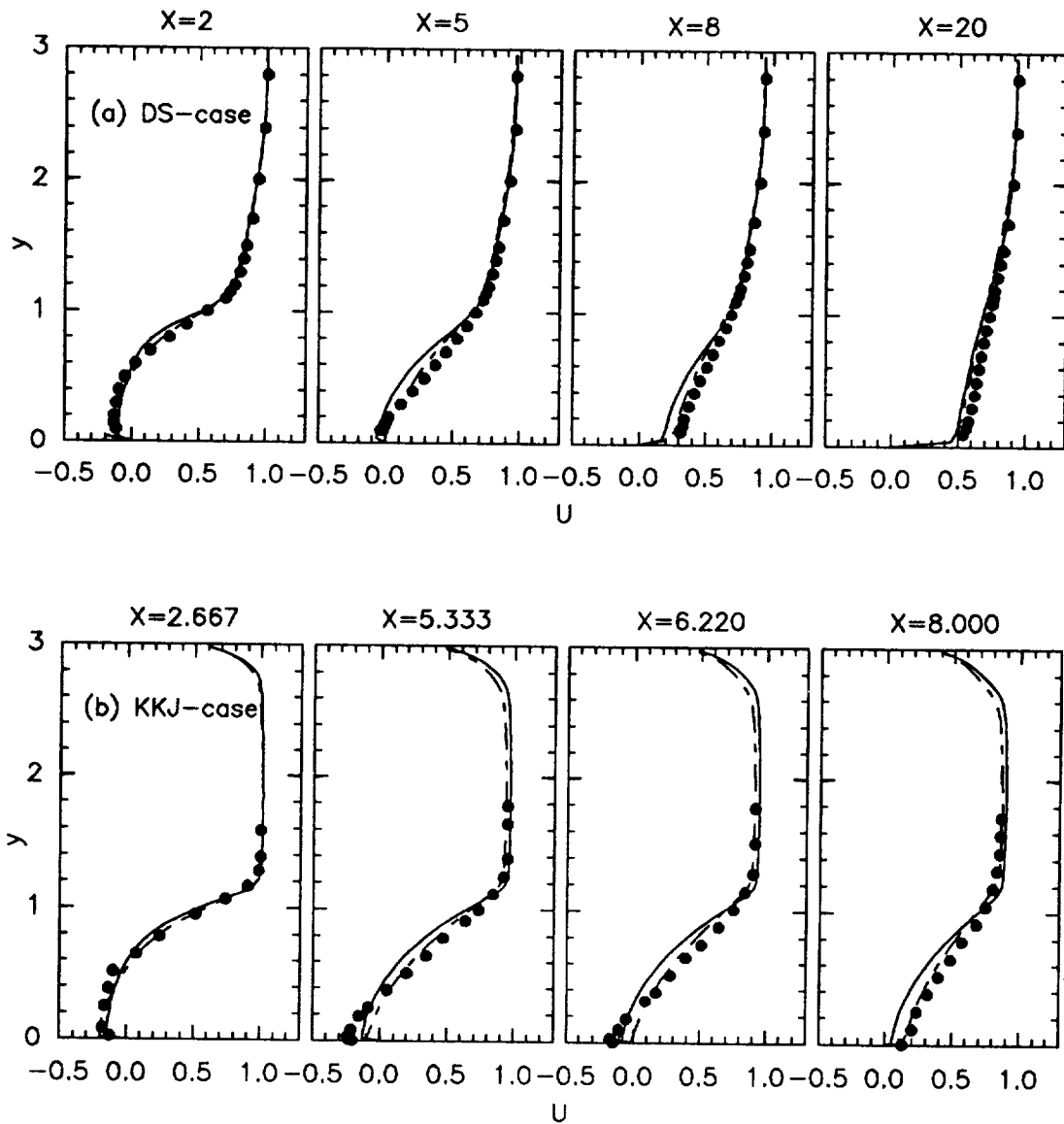


Figure 7. Streamwise mean velocity  $U$ -profiles.  
 - - -: s-K- $\epsilon$ ; —: present model; •: experiment

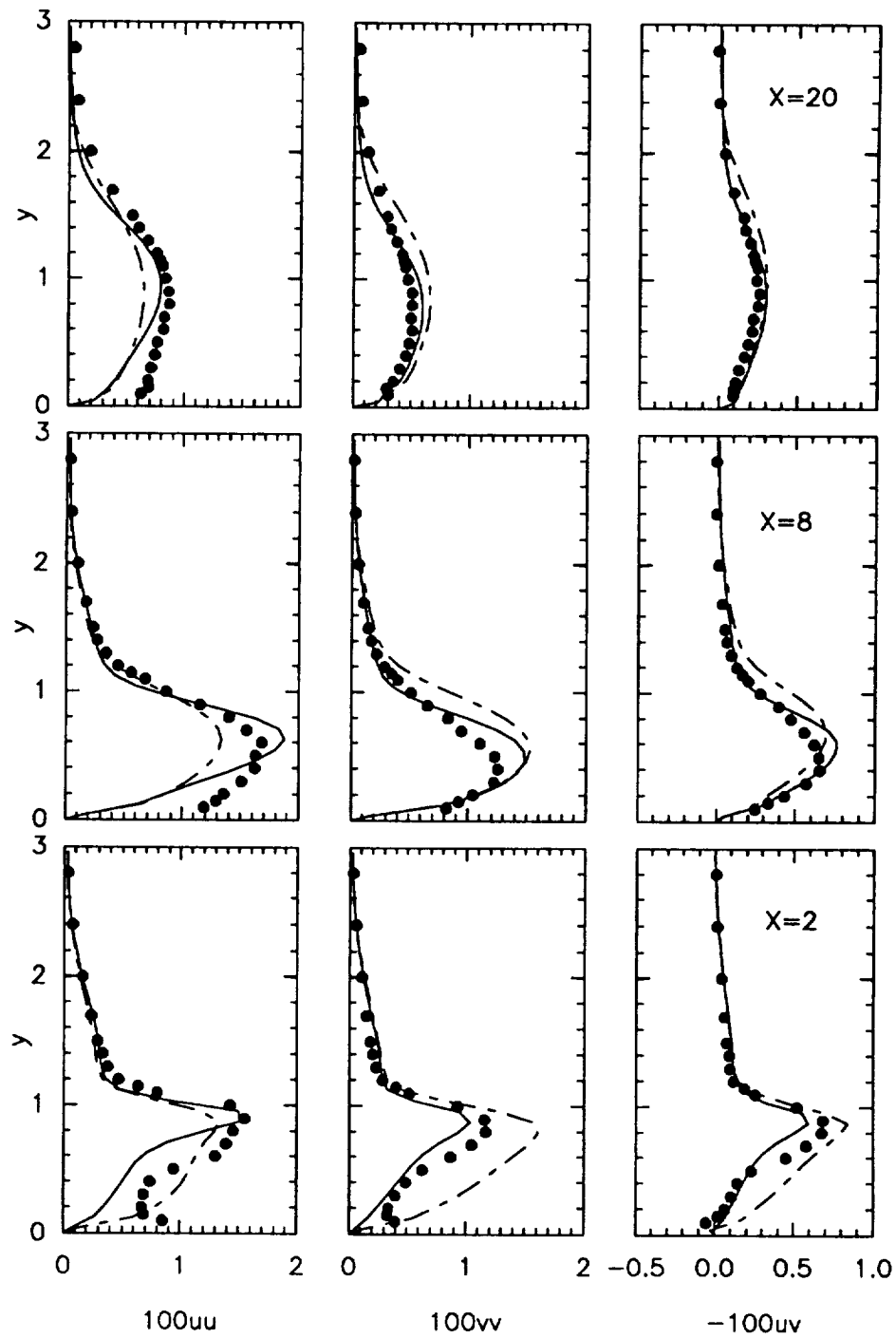


Figure 8. Turbulent stress profiles in DS-case.  
 - - -: s-K- $\epsilon$ ; —: present model; •: experiment

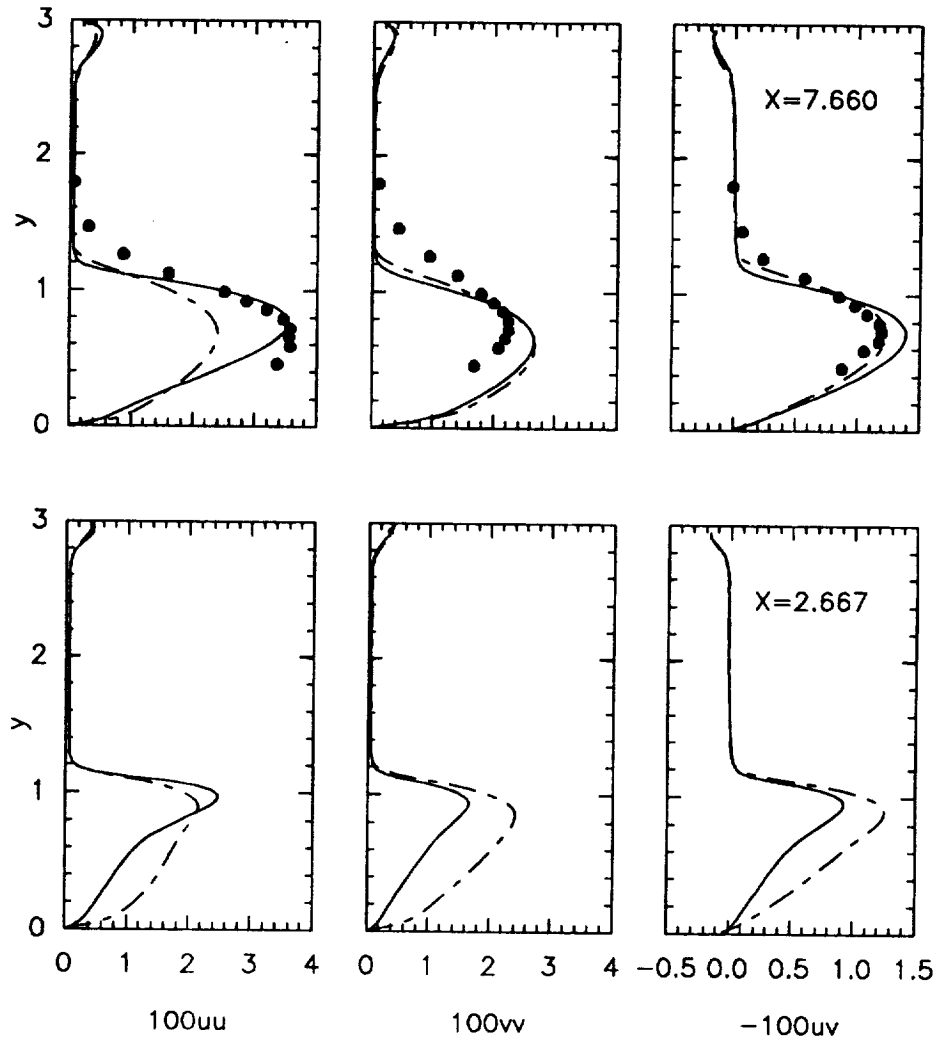


Figure 9. Turbulent stress profiles in KKJ-case.  
 - - -: s-K- $\epsilon$ ; —: present model; •: experiment



# REPORT DOCUMENTATION PAGE

Form Approved  
OMB No. 0704-0188

Public reporting burden for this collection of information is estimated to average 1 hour per response, including the time for reviewing instructions, searching existing data sources, gathering and maintaining the data needed, and completing and reviewing the collection of information. Send comments regarding this burden estimate or any other aspect of this collection of information, including suggestions for reducing this burden, to Washington Headquarters Services, Directorate for Information Operations and Reports, 1215 Jefferson Davis Highway, Suite 1204, Arlington, VA 22202-4302, and to the Office of Management and Budget, Paperwork Reduction Project (0704-0188), Washington, DC 20503.

<b>1. AGENCY USE ONLY (Leave blank)</b>		<b>2. REPORT DATE</b> January 1993	<b>3. REPORT TYPE AND DATES COVERED</b> Technical Memorandum	
<b>4. TITLE AND SUBTITLE</b> A Realizable Reynolds Stress Algebraic Equation Model			<b>5. FUNDING NUMBERS</b>  WU-505-62-21	
<b>6. AUTHOR(S)</b> Tsan-Hsing Shih, Jiang Zhu, and John L. Lumley				
<b>7. PERFORMING ORGANIZATION NAME(S) AND ADDRESS(ES)</b> National Aeronautics and Space Administration Lewis Research Center Cleveland, Ohio 44135-3191			<b>8. PERFORMING ORGANIZATION REPORT NUMBER</b>  E-7525	
<b>9. SPONSORING/MONITORING AGENCY NAMES(S) AND ADDRESS(ES)</b> National Aeronautics and Space Administration Washington, D.C. 20546-0001			<b>10. SPONSORING/MONITORING AGENCY REPORT NUMBER</b> NASA TM-105993 ICOMP-92-27 CMOTT-92-14	
<b>11. SUPPLEMENTARY NOTES</b> Tsan-Hsing Shih and Jiang Zhu, Institute for Computational Mechanics in Propulsion and Center for Modeling of Turbulence and Transition, NASA Lewis Research Center (work funded by Space Act Agreement C-99066-G). Space Act Monitor: Louis A. Povinelli, and John L. Lumley, Cornell University, Ithaca, New York. Responsible person, Tsan-Hsing Shih, (216) 433-5698.				
<b>12a. DISTRIBUTION/AVAILABILITY STATEMENT</b>  Unclassified-Unlimited Subject Category 02			<b>12b. DISTRIBUTION CODE</b>	
<b>13. ABSTRACT (Maximum 200 words)</b> The invariance theory in continuum mechanics is applied to analyze Reynolds stresses in high Reynolds number turbulent flows. The analysis leads to a turbulent constitutive relation that relates the Reynolds stresses to the mean velocity gradients in a more general form in which the classical isotropic eddy viscosity model is just the linear approximation of the general form. On the basis of realizability analysis, a set of model coefficients are obtained which are functions of the time scale ratios of the turbulence to the mean strain rate and the mean rotation rate. The coefficients will ensure the positivity of each component of the mean rotation rate. These coefficients will ensure the positivity of each component of the turbulent kinetic energy - realizability that most existing turbulence models fail to satisfy. Separated flows over backward-facing step configurations are taken as applications. The calculations are performed with a conservative finite-volume method. Grid-independent and numerical diffusion-free solutions are obtained by using differencing schemes of second-order accuracy on sufficiently fine grids. The calculated results are compared in detail with the experimental data for both mean and turbulent quantities. The comparison shows that the present proposal significantly improves the predictive capability of K-ε based two equation models. In addition, the proposed model is able to simulate rotational homogeneous shear flows with large rotation rates which all conventional eddy viscosity models fail to simulate.				
<b>14. SUBJECT TERMS</b> Turbulence modeling			<b>15. NUMBER OF PAGES</b> 36	
			<b>16. PRICE CODE</b> A03	
<b>17. SECURITY CLASSIFICATION OF REPORT</b> Unclassified	<b>18. SECURITY CLASSIFICATION OF THIS PAGE</b> Unclassified	<b>19. SECURITY CLASSIFICATION OF ABSTRACT</b> Unclassified	<b>20. LIMITATION OF ABSTRACT</b>	